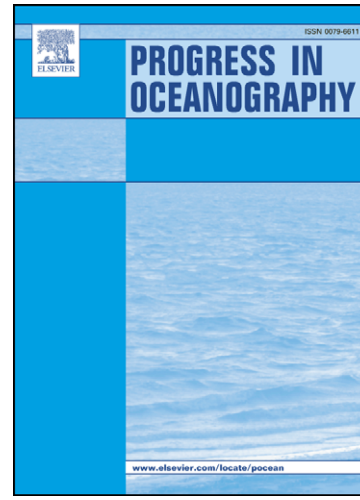

Nutrients in an oligotrophic boundary current: Evidence of a new role for the Leeuwin Current

P.A. Thompson, K. Wild-Allen, M. Lourey, C. Rousseaux, A.M. Waite, M. Feng, L.E. Beckley

PII: S0079-6611(11)00026-7
DOI: 10.1016/j.pocean.2011.02.011
Reference: PROOCE 1087

To appear in: *Progress in Oceanography*

Received Date: 13 October 2010
Revised Date: 18 February 2011
Accepted Date: 18 February 2011

Please cite this article as: Thompson, P.A., Wild-Allen, K., Lourey, M., Rousseaux, C., Waite, A.M., Feng, M., Beckley, L.E., Nutrients in an oligotrophic boundary current: Evidence of a new role for the Leeuwin Current, *Progress in Oceanography* (2011), doi: 10.1016/j.pocean.2011.02.011

Nutrients in an oligotrophic boundary current: Evidence of a new role for the Leeuwin Current.

Thompson, P.A.[1,2] Wild-Allen, K.[1,2] Lourey, M.[1,2] Rousseaux, C.[3] Waite A.M.[3] Feng, M.[1,2] Beckley L.E.[4]

[1]Marine and Atmospheric Research, GPO Box 1538, Hobart TAS, 7001, Australia.

[2]Wealth from Oceans, National Research Flagship.

[3]School of Environmental Systems Engineering, University of Western Australia, 35 Stirling Highway, Crawley, WA 6009, Australia

[4]School of Environmental Science, Murdoch University, South Street, Murdoch, WA, 6150, Australia

Corresponding author:
Peter Thompson
GPO Box 1538
Hobart, Tasmania
7001 Australia
peter.a.thompson@csiro.au
ph 61 3 6232 5298
fax 61 3 6232 5000

Abstract

New observations along the continental shelf of Western Australia provide a novel explanation for the established ~60 y relationship between Leeuwin Current (LC) strength and greater winter nitrate concentrations at 32°S plus the interannual variation in the magnitude of the annual, shelf-scale, phytoplankton bloom. The potential source of dissolved nitrogen to support the annual shelf scale phytoplankton bloom was identified as thin layers of an unprecedented areal extent, nitrate concentration and shallow nature that were observed off the northwest of Australia. We propose that the dissolved inorganic nitrogen (DIN) in these layers enters the LC at depth and then enters the euphotic zone via by three mechanisms: instability that results in a warm core eddy, cooling that deepens the surface mixed layer and shallowing of the thin layer. During the onset of the annual phytoplankton bloom along the west coast of Australia from 22°S to 34°S the poleward flowing LC was clearly evident as a surface intensified ocean boundary current transporting warmer, lower-salinity, greater-silicate waters in a shallow mixed layer rapidly southward. Between 24 and 26°S the core of the LC was present as a 50 to 100 m deep layer over one or more thin layers, 15 to 50m thick, with high nitrate and low dissolved oxygen (DO). These layers were of lower salinity, cooler water with markedly reduced DO, high nitrate concentrations and distinct nitrate:silicate (NO_3:$Si(OH)_4$) nutrient ratios. As the LC flowed south it cooled and deepened thereby entraining the thin layers of high nitrate water into the euphotic zone. The LC also formed large (greater than 100km diameter) warm core eddies with a deep surface mixed layer that also entrained nitrate from these thin layers. In some locations as far south as 32°S the LC was still present with the thin layer of high nitrate intact but now within the euphotic zone. Thus, the available evidence suggests the LC arises under conditions that favour rapid and shallow nitrification. This nitrification fuels a shelf scale bloom on a downwelling favourable coast. Depending upon the rate of nitrification the source of the particular organic matter may be local or delivered from the tropics via horizontal advection in a subsurface layer of the LC.

Key words: nutrients; phytoplankton bloom; Australia; nitrification; eddy; vertical mixing; thin layers.

Introduction

The central gyre of the Indian Ocean from 5 to 45°S is amongst the world's most oligotrophic regions with a very low standing stock of phytoplankton (Polovina et al. 2008). Previous phytoplankton ecologists have indeed described the eastern Indian Ocean as a desert (Wood 1964). The region of the eastern Indian Ocean along the west coast of Australia experiences a midwinter peak in phytoplankton biomass (a bloom in the desert) that spans more than 15° of latitude and extends from the coast to several hundred km offshore (Moore et al. 2007). The source of nutrients to support this bloom has been the subject of considerable debate with several hypotheses being advanced (Feng et al. 2009) including transport (Koslow et al. 2008) in the Leeuwin Current ([1]LC), a coastal source (Dietz et al. 2009), upwelling (Hanson et al. 2005), deep mixing associated with eddy formation (Waite et al. 2007), or seasonal cooling that results in deepening of the seasonal thermocline and the entrainment of more nitrate into the euphotic zone (Koslow et al. 2008). The magnitude of the annual west coast bloom is known to vary in proportion to the strength of the Southern Oscillation Index (Thompson et al. 2009) as does the strength of the Leeuwin Current (Feng et al. 2003); both are greater during La Niña events. These spatial and temporal patterns of variations in nutrients and phytoplankton suggest that the strengthening LC somehow delivers more nutrients into the euphotic zone.

The Leeuwin Current arises due to geostrophic transport from the Indonesian Throughflow that generates an alongshore steric height gradient, sufficient to overcome the equatorward wind stress and suppress the Ekman driven upwelling, thus limiting the supply of nutrients to the surface waters (Pearce, 1991). Off the west coast of Australia the buoyant Leeuwin Current (LC) flows strongly poleward at the surface along the shelf break, peaking at 7 Sv in midwinter (Feng et al.

---

[1] Abbreviations: Leeuwin Current (LC), low dissolved oxygen and high nitrate (LDOHN), dissolved inorganic nitrogen (DIN), particulate organic matter (POM), organic matter (OM), warm core (WC), cold core (CC), . diadinoxanthin (DD), diatoxanthin (DT), fluorescence (Fl).

2003) and covering much of the region with a thin layer of warm, relatively fresh water. Relative to the surrounding waters the LC carries greater concentrations of silicate and phosphate but concentrations of dissolved inorganic nitrogen (DIN) remain low through winter (Johannes et al. 1994, Lourey et al. 2006) suggesting that the growth of phytoplankton in these shelf waters is limited by the availability of N.

Previous evidence for upwelling along the west coast of Australia is restricted to one location and one time of the year. In the SW corner of the continent during the summer period, when the Leeuwin Current is nearly nonexistent, strong northward winds can drive a cold Capes Current from the Capes Leeuwin and Naturaliste region (Pearce and Pattiaratchi, 1999). Localized Ekman-driven upwelling of cold deep water associated with the Capes Current is hypothesized as the basis of some localized increase in primary production (Gersbach et al. 1999, Hanson et al. 2005). There is little evidence for upwelling along other regions of the west Australian coast although it has been suggested as a possible mechanism responsible for the sporadically high rates of primary production observed at ~ 25°S (Hanson et al. 2005).

At mid latitudes (~ 32°S) increased phytoplankton biomass and primary production were observed in deeply mixed warm core eddies (Thompson et al. 2007). The source of nitrogen to support these productive warm cores eddies was hypothesized to be entrainment from coastal waters (Greenwood et al. 2007, Dietz et al. 2009) or eddy induced upwelling (Waite et al. 2007). Previous studies of mesoscale variation off the west coast of Australia identified newly forming eddies to contain more nitrate in the euphotic zone (Paterson et al. 2008) and for mature eddies to contain greater phytoplankton biomass (Moore et al. 2007). Some component of the inter-annual variability in regional productivity must be associated with the greater mesoscale eddy energy during La Niña years (Fang and Morrow 2003, Feng et al. 2005) as a single WC eddy represents an increase of ~6000 tons in particulate organic carbon (Feng et al. 2007). The winter shelf (Thompson and Waite 2003) and eddy microplankton (Thompson et al. 2007) tend to be diatom dominated, a characteristic often associated with relatively deep mixing, low average irradiances and nitrate as the nitrogen source (Lomas and Glibert 1999, 2000, Litchman and Klausmeier 2001, Litchman et al. 2004).

At most locations around the world the average winter nitrate concentration is negatively correlated with sea surface temperature (e.g. Switzer et al. 2003, Kamykowski and Zentara 1985), but this is not true for west Australian shelf waters where warmer winter temperatures are associated with greater surface nitrate concentrations (Thompson et al. 2009). In most of the world's oceans convective cooling and increased wind during winter acts to deepen the seasonal thermocline and resupply the euphotic zone with nutrients including nitrate (Kamykowski and Zentara 1985). Off most of west Australia, however, the annual amplitude in the depth of the mixed layer reported to be only 10 m (Condie and Dunn 2006) which is a remarkably small seasonal deepening of the seasonal thermocline relative to these latitudes on the east coast of Australia (Condie and Dunn 2006) or the 100 m found in some regions of the ocean (Sprintall and Roemmich 1999). This small amplitude in mixed layer depth (MLD) may be associated with the winter flow of the buoyant LC.

In this study we undertook a shelf scale survey off Western Australia during the period when Leeuwin Current flow was increasing and the annual primary production cycle was nearing its peak (May-June). In our search for the nutrient source to support this bloom we increased the spatial resolution of sampling relative to any previous research along this coast. Bottle samples for nutrient analysis were obtained at relatively narrow depth increments (≥10m). Ultraviolet spectrophotometric detection of nitrate concentrations (Johnston and Coletti 2002) were undertaken as a component of most CTD casts giving ~ 1 estimate of nitrate concentration m^{-1}. Cross-shelf sections of temperature, salinity, fluorescence, dissolved oxygen and transmission were collected via a towed, undulating CTD system. The nutrient concentrations in the euphotic zone (0 – 100m) were examined and regions of greater concentrations investigated in detail for potential sources and mechanisms of injection. Potential links between surface mixed layer nitrate concentrations and vertical mixing were investigated by considering the degree of stratification and evidence that the surface mixed layer was actively mixing.

Based upon the results a description of the processes that deliver dissolved inorganic nitrogen into the euphotic zone along the continental shelf off western Australia was developed (Fig. 1). The results indicate the presence of a shallow layer of low dissolved oxygen and high nitrate water offshore and just below the high phytoplankton biomass found in the surface mixed layer of the LC between 22 to 25°S (Fig. 1). This layer is transported south along the base of the LC (Woo and Pattiaratchi 2008). Southwards and near the Abrolhos Islands the Leeuwin Current narrows developing high eddy kinetic energy (Feng et al. 2005). South of the Abrolhos Islands the LC produced a large warm core eddy observed off the shelf at ~ 31°S with relatively high nitrate and low dissolved oxygen plus N:Si ratios. These characteristics are indicative of the nitrate in the eddy resulting from entrainment of the layer from the base of the LC. The LC cools as it progresses southwards and further south, off Perth (~32°S), the LC existed in 2 modes. One mode with nitrate from this thin layer mixed throughout the surface mixed layer (purple colour) and another with the thin layer still intact but at relatively shallow depths (~ 70m).

Materials and Methods

Physics

Onshore – offshore transects were conducted along each degree of latitude from 34°S to 22°S along the west coast of Australia. In general CTD profiles were obtained at water depths of 25, 50, 75, 100, 200, 300, 500, 750, 1000, and 2000 m on each transect, with at least one station positioned to be in the middle of the LC. A total of 111 stations were vertically profiled during the cruise using a Seabird SBE 911 instrument (CTD) to measure conductivity (converted to practical salinity units), pressure (converted to depth [m]) and temperature (°C). Most vertical profiles also contained photosynthetically active radiation (PAR, 400 to 700 nm, Biospherical Instruments QCP-2300), fluorescence (Chelsea Instruments Aquatracka™ fluorometer), % transmission (Wetlabs C–Star™), dissolved oxygen (Anderra 3975 series optode) and nitrate (Satlanic ISUS sensor) concentrations.

The Seabird 911 conductivity sensor was validated against 184 bottle samples analysed for salinity and showed a small standard deviation of 0.002 PSU. These data were then averaged over 2m depth increments. Mixed layer depth was calculated using temperature and salinity (after Condie and Dunn 2006) as the depth at which the temperature was 0.4°C less than that observed at 10m or salinity was 0.03 more than that measured at 10m. At each CTD station the mixed layer depth was the shallower of these two. From each CTD profile the gradients in temperature, salinity, dissolved oxygen, fluorescence and percent transmission were calculated from 0 to 50m, 50 to 100m and 100 to 150m. These gradients between different parameters were examined for associations (Pearson correlations) that might reflect consistency in vertical structure between parameters. They were also assessed for association with nitrate in the euphotic zone.

A towed undulating body (Seasoar) was used to provide high resolution sections across the Leeuwin Current. A typical undulation was ~ 150m requiring about 6 minutes and over a single transect across the LC provided hundreds of vertical profiles for temperature, salinity, dissolved oxygen, fluorescence and % transmission. The majority of transects between the inshore station at one latitude and the offshore start of another set of CTD stations along the next fixed latitude were surveyed by Seasoar, for example, the 150 km transect between the inshore station at 34°S (114.9°E) and the offshore station at 33°S (113.8°E). Continuous underway data recorded on the vessel, RV *Southern Surveyor*, included surface PAR, wind speed, direction, surface temperature, salinity, fluorescence, bottom depth and ADCP measured current velocities from a vessel mounted RDI 70 kHz Ocean Surveyor Acoustic Doppler Current Profiler (ADCP) (Teledyne RD Instruments). The instrument was set to record from just below the ship (~ 10m) to a maximum water column depth of 300 m and data were averaged in 8 m depth bins.

Chemistry

Bottle samples (n ~ 851) from multiple depths (range 0 to 1949m) from 111 CTD casts were analyzed for nitrate, nitrite, ammonium, silicate and phosphate concentrations using Quick-Chem™ methods on a flow injection LACHAT® instrument as per the following protocols for nitrate + nitrite (Quik-Chem™ Method 31-107-04-1-A; detection limit ~0.03 µM; adapted from Wood et al. 1967), silicon (Quik-Chem™ Method 31-114-27-1-D; detection limit ~0.05 µM; adapted from Murphy and Riley 1962) and phosphate (Quik-Chem™ Method 31-115-01-1-G; detection limit ~0.02 µM; adapted from Armstrong 1951). Samples were analyzed for ammonium on the LACHAT® instrument using the technique of Kerouel and Aminot (1997) adapted for flow injection, detection limit ~ 0.05 µM. The Satlantic ISUS™ sensor was included on CTD profiles < 1000m. Up-cast nitrate profiles derived from in-situ ultraviolet spectrometry (IN) were calibrated against bottle samples (BN) [$BN = 1.22IN – 0.29$; $r^2 = 0.92$], and were corrected for temperature dependant hysteresis (Johnson and Coletti 2002) and individual cast offsets likely associated with thermal shock and/or false blank (dark voltage) on deployment.

Dissolved oxygen (DO) concentrations from 162 bottle samples were measured by automated Winkler titration on a Metrohm 765 Dosimat™. These were compared with the Aanderra model 3975 optode fitted to the CTD system. In general the optode showed good agreement with the chemically determined concentrations (Fig. 2A). In particular the optode sensor did not underestimate chemically measured DO. A few chemical measurements were lower than those estimated by the sensor and these were not used in the calibrating the sensor. This early model optode had quite slow response times and possibly due to the thin layers of low DO water (sometimes less than 10m thick) there may not have been sufficient time for equilibrium at the vertical velocity 1 m s^{-1} normally used during a CTD profile. In some regions narrow layers of low dissolved oxygen were at relatively shallow depths and most often below a strong pycnocline. In these regions the observed concentration of dissolved oxygen was compared with the solubility of oxygen for the prevailing conditions of temperature and salinity after Garcia and Gordon (1992). The solubility concentration (DO*) minus the observed concentration = subsaturation. For the purpose of assessing the respiration represented by this subsaturation as a potential source of nitrogen the organic matter (OM) was assumed to have 1:1 and 6.6:1 ratios for O:C and O:N, respectively (Fraga et al. 1998) and the apparent oxygen utilization (AOU = theoretical 0_2 solubility - observed O_2 concentration) was calculated from the classic "Redfield model" (Redfield, 1942). Over the depth range of 0 – 100 meters the agreement between observed nitrate (bottle samples) and potential nitrate concentrations estimated from the respiration of OM by this method was reasonable (r^2 = 0.48), especially at concentrations greater than 0.3 µM nitrate (Fig. 2B). The slope of 1.71± 0.08 (P < 0.001) suggests at least 60% of the potential N remineralized over these depths was present in the water column as nitrate.

Biology

A variable number of stations was sampled for biological parameters in a manner designed to give approximately consistent cover of three regions at each degree of latitude. The regions were defined as inshore of the Leeuwin Current (~ 50m deep), in the centre of the Leeuwin Current (~ 200 to 300m deep) and offshore (1000 or 2000m deep). Fifty four stations and 6 depths (n = 520) from 0 to < 300 m were sampled and 2 size fractions (greater than 0.7 µm, collected on Whatman GF/F™ filters and greater than 5 µm, collected on 5µm Nitex™ mesh) were extracted in 90% acetone overnight at -20°C and analysed for chl*a* on a calibrated Turner Designs model 10 AU fluorometer (Parsons et al. 1984).

Two size fractions (less than 5 m and greater than 5 micron) were collected from three stations per latitude and 2 depths per station for analysed by HPLC to determine a suite of pigments using Waters® instrumentation (a Waters 996 Photodiode Array Detector, a Waters 600 Controller, and a Waters 717plus Autosampler). The HPLC system used an SGE 250 x 4.6 mm SS Exsil ODS (octodecyl silica) 5 µm column. Pigments were eluted over a 30 minute period with a flow rate of 1 ml min^{-1}. The Van Heukelem and Thomas (2001) method was used which gave improved resolution to chlorophylls c_1 and c_2, and full resolution of MV and DV chlorophylls *a* and *b,* lutein and zeaxanthin. Each solvent was pre-filtered through a Millipore HVLP 0.45 µm filter. The separated pigments were detected at 436 nm and identified against standard spectra using Empower™ software. Concentrations of the pigments were determined from standards (Sigma® and purified pigments obtained from algal cultures).

<u>Rates of vertical mixing.</u>

Typically wind stress or surface cooling are the major forces that increase mixing, weaken stratification and can increase the vertical transfer of nutrients into the euphotic zone. As pointed out by Huisman et al. (1999), however, even with vertical gradients in physical parameters that are small enough for a layer to be defined as mixed, the rate of vertical mixing can be so slow that chemical and biological gradients develop. Therefore the vertical gradients were assessed using temperature, salinity, DO, chl*a* fluorescence and phytoplankton pigments. The latter approach uses the physiological adjustment of phytoplankton to light as a very sensitive method to assess rapid vertical mixing. Cells rapidly adjust their cell quota of photoprotective pigments in response to variation in irradiance, or depth, and these pigments can be used to estimate how long cells have been away from the surface. Normalizing to chl*a* improves the precision of the estimate (Claustre et al. 1994, Moline 1998). The intracellular concentration of the photoprotective pigments diadinoxanthin (DD) and diatoxanthin (DT) photoacclimate on a time scale of minutes to hours (Brunet et al. 2003). If the rate of vertical mixing is relatively rapid then the observed difference (DD+DT)/chl*a* over a change in depth (Δz) will be small relative to changes observed in a more stable water column. The vertical displacement velocity in the euphotic zone can be calculated from:

$$\frac{\Delta z}{\Delta t} = \frac{\Delta z(-k)}{\ln\left[(R_t - R_\infty)/(R_0 - R_\infty)\right]} \qquad \text{eqn. 3.}$$

where k is the first-order rate constant for the photoacclimation parameter of choice, R_t is the parameter at time t, R_0 is the same parameter at time zero, R_∞ is the parameter after an infinite time of photoacclimation, and Δz is the vertical distance between the surface and the depth of 1% surface irradiance (after Falkowski 1983). For the purpose of calculating mixing rates the lowest observed value of (DD+DT):MVchl*a* was selected as R_∞. A k value of 0.5 h^{-1} was adopted from the literature (Claustre et al. 1994, Moline 1998, Brunet et al. 2003).

Results

Background and study area

The cruise commenced on May 15th 2007 just prior to the onset of austral winter and, as anticipated, we sampled as the regional phytoplankton bloom approached its annual maximum (Fig 3, inset C). Relative to climatology, the phytoplankton bloom in 2007 in the study region (111 to 116°E and 35 to 21°S) was 30% less than normal (1997-2010). Shipboard ADCP showed considerable current velocities (~ 1 m s^{-1}) along the entire coast, mostly in the southward direction, but strong northwards flow were observed in some locations (Fig. 3B). Remotely sensed estimates of sea surface height and sea surface temperature showed the LC flowing southward at this time and the presence of anticyclonic (warm core) eddies at ~23, 28, 31 and 34°S (Fig. 3A). Daily updates from remote sensing were used to aid navigation during the research voyage including the facilitation of a complete east-to-west transect through the large warm core eddy between 31 and 32°S.

General overview of nutrient results

Positive outliers of nitrate, nitrite and ammonium concentrations (from bottle samples obtained from the 111 CTD casts) from within the euphotic zone (~ 0 to 100m) and depth averaged (0 to 100 m) were used to identify areas where significant nutrient concentrations intruded into the euphotic zone. Further analysis of the environment, including several methods of estimating vertical mixing, were used to investigate potential mechanisms that might supply this dissolved nitrogen to the euphotic zone. Nitrate was the most abundant dissolved inorganic N species. Over all depths (0 to 2000m) the average nitrate concentration was 3.0 µM followed by 0.15 µM for ammonium and 0.08 µM for nitrite. Over the entire cruise, but restricted to the euphotic zone (defined here as 0 to 100m), the average ± SD nitrate (NO_3), silicate ($Si(OH)_4$) and phosphate (PO_4) concentrations were 0.26 ± 0.46 (n = 550), 2.42 ± 0.71 (n = 531) and 0.076 ± 0.046 µM (n = 536), respectively. Nutrient concentrations tended to covary with depth and with each other; NO_3, $Si(OH)_4$ and PO_4 reaching greater than 30, 100 and 2 µM, respectively, at 1000 m (Fig. 4). The relative availability of dissolved macronutrients deviated significantly from the Redfield (1963) ratios of 16:16:1 (N:Si:P) required by phytoplankton. The excess of $Si(OH)_4$ over NO_3 was considerable, and over all depths, only 11% of samples had N:Si ratios greater than Redfield (greater than 1) while 63% of all measurements were < 0.1 or less than Redfield by a factor of 10 (Fig. 4). In the case of PO_4 the excess relative to NO_3 was still extreme, albeit differently distributed. Only 0.6% of all measurements exceeded Redfield (N:P greater than 16) while 34% of all measurements were 10 times less than Redfield (Fig. 4). The average euphotic zone nitrate concentration (0.26 μM) and ratios for dissolved inorganic NO_3:$Si(OH)_4$:PO_4 of ~ 3:30:1 suggest the likelihood of extreme N limitation with both Si and P available to phytoplankton in relative excess. The euphotic zone had just 20 measurements, or 3.8% of all observations, of ≥1 μM nitrate. These locations are investigated further below.

<u>North to south description of nutrient sources in the Leeuwin Current</u>

Several features of the LC are described in detail to elucidate the important sources of nutrients and the processes that deliver these to the euphotic zone. At 22°S the continental shelf is very narrow with a prominent low DO layer observed at ~ 175m depth (Fig. 5). This low DO was associated with low salinity water and markedly elevated nitrate concentrations (~8μM) relative to the water above (mean bottle samples NO_3 = 0.15 μM ±0.08). Below this low DO layer, the nitrate concentration went through a minimum at 250m before increasing again at depths exceeding 350m. At 22°S the surface mixed layer was relatively deep (Fig 6C) at the shelf break, considerably deeper than the approximately 40m at 23°S and most locations further south. High rates of vertical mixing were implied by the lack of photoacclimation in photoprotective pigments especially at 22°S (Fig. 6C). The satellite altimetry data reveal the presence of a nearshore, cyclonic or cold-core (CC) eddy at 22°S at the time of sampling (Fig. 3A) a likely factor in accelerating the LC and the deepening of the mixed layer. The surface 150m had a NO_3:Si ratio of ~0.03 that increased to 0.77 in the low salinity, high nitrate layer found at ~150 m. The phytoplankton within the eddy at 22°S were deeply mixed reaching nearly 170m.

Evidence of thin, shallow layers of low dissolved oxygen and high nitrate off northwest Australia

At the offshore end (≥ 1000m depth) of the 3 transects at 23, 24 and 25°S there was considerable nitrate (~ 5 µM) present relatively deep (50 to 100m) in the euphotic zone (Fig. 6A, 7). Here the Leeuwin Current (LC) was strongly evident as a warm (approximately 25°C), low salinity (35.2 psu) and high chl*a* (fluorescence) water mass from the surface to approximately 85m at 24°S (station 94, Fig. 7). This surface layer of high velocity, warm, low salinity water is considered as the defining feature or core of the LC. Further south at 25°S and still offshore the LC had similar T, S and Fl characteristics but was shallower reaching only to a depth of approximately 50m at 25°S (station 88, Fig. 7). Sharp temperature, salinity, fluorescence, dissolved oxygen (DO) and nutrient gradients were present and below this layer there was a cooler and fresher layer with low DO and high nitrate. At 24°S (Stn 94), and especially at 25°S (Stn 88), it was evident that the concentrations of nitrate did not increase uniformly with depth in association with decreasing temperature and increasing salinity (Fig. 7). At station 94 nitrate concentrations reached 8.8 µM at 160m. Nitrate concentrations fell with depth to a minimum at approximately 250m and then rose steadily towards the seafloor (Fig. 7). At station 88 the nitrate concentrations were 5.5 µM at 88m, declined to near zero before a second peak at 205m, declined again towards 250m before eventually rising with depth. The horizontal layering of waters with distinct differences in density and fluorescence, nitrate and DO strongly suggest that the greater nitrate concentrations in these layers were not generated by vertical mixing from greater depth.

Forms of dissolved inorganic nitrogen in the euphotic zone and their potential sources

The availability of dissolved inorganic nitrogen to phytoplankton in the euphotic zone at stations 88 and 94 could be assessed from the 6 bottle samples analysed for nutrients between 0 and 100m. At station 88 the depth-averaged nitrate was 0.92±2.2 µM while nitrite was 0.04±0.07 µM and ammonium was 0.01±0.009 µM. Similarly, at station 94 depth-averaged nitrate was 1.0±2.2 µM while nitrite was 0.01±0.01 µM and ammonium was 0.007±0.005 µM. Thus nitrate was 25 to 100 times more abundant than nitrite or ammonium in the euphotic zone and was a potential source of DIN for phytoplankton growth in this northern region.

All of the shallow layers of unusually high nitrate were closely associated with a decline in DO. The bottle samples analysed for nitrate showed very good agreement with the concentrations estimated by the ISUS sensor but the vertical resolution achieved by the latter made the relationships between DO and nitrate much more evident in these relatively thin layers. For these profiles the apparent oxygen utilization (AOU = theoretical O_2 solubility - observed O_2 concentration) was calculated from the classic "Redfield model" (Redfield, 1942). Theoretical solubility was calculated after Garcia and Gordon (1992). These AOUs were then converted into potential DIN assuming respiration of phytoplankton biomass with Redfield (Redfield 1942) ratios of C:N and O:C of 1:1 (Fraga et al. 1998). The predicted DIN concentrations closely replicate the vertical patterns in nitrate concentrations with only minor overestimations in DIN relative to the measured nitrate values (Fig 7). Thus these relatively shallow (75 to 150 m) peaks in nitrate concentrations were potentially generated by particulate organic matter (POM) remineralized near the base of the LC.

Depth-averaged, euphotic zone nitrate concentrations showed a strong pattern of greatest concentrations along the shelf break with lower concentrations found closer to shore or further offshore (Fig. 6A). These shelf break stations were selected to coincide with the centre of the LC as determined from Seasoar sections and real time underway surface data. The shelf break stations had depth-averaged euphotic zone (0 to 100m) nitrate concentrations consistently in the range of 0.15 to 0.30 µM NO_3 in the vicinity of the LC. Based on the salinity and temperature derived estimates of mixed layer depth these shelf break stations with greater depth-averaged nitrate concentrations (Fig. 6A) were generally not areas of particularly deep vertical mixing (Fig. 6C). Due to the presence of the LC along the shelf break between 23 and 33°S the mixed layer depths were mostly quite shallow averaging ~ 40 to 60m. In general a surface mixed layer depth of 60m is not sufficient to entrain nutrients from below the seasonal thermocline in these locations.

Greater ammonium concentrations at mid coast latitudes as evidence for a change in processes.

Over the entire cruise and within the euphotic zone (0 to 100m) ammonium was rarely (only 13 of 405 measurements) observed at concentrations exceeding 1µM. These few observations of greater than 1µM ammonium resulted in depth-averaged values (0 to 100m) exceeding 0.3 µM NH_4

between 29 and 32°S and 113 to 114.5°E (Fig 6B). For example at 31°S and in 1000m water the euphotic zone (0 to 100m) had a depth-averaged concentration of 0.78 µM NH_4 and 2 measurements of greater than 1 µM NH_4 (Fig. 7, station 49). At this offshore location the euphotic zone nitrate concentrations were also elevated relative to inshore and relatively constant from 0 to 100m at 0.33±0.02 µM. The LC was present as a deeper (~ 125m) isothermal and isohaline feature that was significantly cooler and saltier than further north.

Vertical mixing as a factor in nitrogen supply to the euphotic zone.

In general there were very strong vertical gradients in biogeochemical parameters observed at the base of surface mixed layer (Fig. 7) indicating that rates of vertical mixing to greater depths were slow relative to phytoplankton growth and nutrient remineralization. Over the duration of the cruise the observed nitrate minima were always deeper than the surface mixed layer (Fig. 7, 8). Even the deepest surface mixed layers with eddies remained isolated by density gradients from the nitrate below the seasonal thermocline (see later). Vertical gradients from the surface to 50 m were relatively weak in all parameters at only a few isolated locations: at 22°S (eddy), offshore at 23°S and the eddy at 31°S. Over the entire research voyage the strength of vertical gradients in temperature, salinity, DO, fluorescence and percent transmission over 0 to 50m, 50 to 100m and 100 to 150m were highly correlated (Table 1). In particular the strength of the fluorescence gradient was correlated with the gradient in % transmission ($P = 2x10^{-17}$). Fluorescence gradients were also positively correlated with temperature gradients but negatively with salinity gradients suggesting that fresher, warmer waters at the surface were important factors for the initiation of this shelf scale bloom (Table 1).These gradient results and their interpretation as indicators of vertical mixing were broadly consistent with those estimated from (DT+DD)/chla. There were relatively few stations where, based on the ratio of (DT+DD/chla), rates of vertical mixing were rapid, ~ 10 cm s^{-1} between the chl*a* maximum and the surface (Fig. 6C). These relatively high rates of vertical mixing between the surface and deep chl*a* maximum (DCM) were only observed where the DCM was within the surface mixed layer. For example, in the LC between 22 and 24°S and at 33 and 34°S) and in the eddies at 22°S and 31°S . Excluding the warm core eddy at 31°S (see later) there was relatively little coherence in the patterns of elevated euphotic zone nitrate concentrations and observations of relatively rapid vertical mixing (Fig. 6A, B, C) between the chl*a* maximum and the surface.

The warm core eddy at ~ 31°S and its potential sources of dissolved inorganic nitrogen.

A significant deepening of the surface mixed layer was observed in the LC meander that was forming a warm core (WC) eddy during the early portion of the cruise. This feature had formed a detached eddy and was moving south east at ~ 7 km d^{-1} between 16/05/2007 and 31/05/2007. We sampled across this eddy on 22/05/2007 at 31°S and 112.7°E where the mixed layer depth reached ~ 160m. This newly formed and strongly rotating feature with a diameter of greater than 100 km was slightly less saline and slight colder than core LC water and had a much deeper surface mixed layer depth than the surrounding water masses (Fig. 6B). Within this eddy a very large injection of nitrate into the euphotic zone had occurred. Relative to the surrounding non-LC water the eddy was warm, fresh, had high concentrations of nitrate and low concentrations of dissolved oxygen (Fig. 8). The adjacent surface waters had nitrate concentrations ranging from 0.1 µM to below detection limit while across the eddy surface nitrate was 0.42 to 0.80 µM. Reflecting the general surplus of Si over N along the west coast of Australia both the surface LC and adjacent surface mixed layer had low molar NO_3:Si ratios with an average of 0.03 over 0 – 50m. Shoreward of the LC there was no source of nitrate (Fig. 8). In sharp contrast the WC eddy had NO_3:Si ratios about 10 times greater, ~ 0.25. The core of the LC upstream of the eddy also had NO_3:Si ratios a long way below 0.25. Based upon our observations it is not possible to create a WC eddy with these N:Si and DO characteristics using water derived from shoreward of the Leeuwin Current (i.e. coastal), from the core of the LC or from any other shallow water mass in the vicinity of the eddy. Underneath the eddy there are water masses with greater nitrate concentrations and high N:Si ratios but there is a very significant density gradient between these and the eddy suggesting vertical mixing is not very significant. Relative to the WC eddy at 31°S with its relatively high nitrate and low DO, the eddy observed at 22°S had these characteristics mostly isolated below it

High resolution sections just upstream of the 31°S eddy show the LC was not homogenous but consisted of multiple ‘streams’ of differing characteristics (Fig. 9). The surface mixed layer was

~ 100m deep and centred at ~ 113.8°E. Below this was a thin layer of intermediate salinity and low DO between 100 and 150 m (Fig. 9). This thin layer was similar to the low DO, high nitrate, unusual NO_3:Si observed just below the surface layer of the LC at 23, 24 and 25°S (Fig. 6). The thin layer was modestly cooler and fresher than the water above or below it (Fig. 6, 9). The high resolution sections obtained by Seasoar show this to feature to be constrained to immediately below the core of the LC between 29 and 30°S and not an intruding water mass from onshore or offshore (Fig. 9). The Seasoar section also shows a very high degree of spatial variability in the phytoplankton biomass (Fig. 9). Outside the LC and offshore there is a deep chl*a* maximum at ~ 75m. Moving across the LC the principal orientation of spatial variability within the euphotic zone is no longer vertical but has become strongly horizontal. Therefore, within the relatively homogenous surface mixed layer of the LC the distribution of phytoplankton biomass shows considerably more horizontal structure than further offshore.

Evidence for a range of nitrogen pathways into the euphotic zone in the southwest.

Considering a longitudinal section along the shelf break (200 to 300m), approximately the middle of the LC, at 22°S LC salinity was less than 35.2 and the temperature greater than 25.3°C at the surface (Fig. 10). By the time the LC reached 34°S it had cooled approximately 4°C to 21.5°C and increased its salinity by 0.5 to greater than 35.7. This section along the LC also shows the mixed layer depth was shallowest at 26°S and increased north and south of this latitude. It is clear that the LC had lost enough heat and gained enough salt to become similar in density to the water immediately below it at latitudes exceeding 26°S (Fig. 10). As the LC erodes into the thin layer of high nitrate water immediately below these nutrients are mixed higher into the euphotic zone. Thus the main source of the nitrate in the euphotic zone of the LC water south of 28° and the source of the nitrate and low DO in the eddy seems likely to be the entrainment of this deeper water into the surface mixed layer of the LC.

At most sections south of 28°S the deeper LC showed modestly enhanced concentrations of nitrate throughout the surface mixed layer. Some locations, however, retained the structure of a thin, shallow layer of high nitrate and low DO even as far south as 32°S (Fig. 11). At this latitude the section shows a thin layer of high nitrate, low DO that is below a very weak salinity and temperature induced density gradient (0.1 ppt and 0.1°C). At ~ 70m this nitrate is within the euphotic zone. South of 28°S and near the Abrolhos Islands there was also broad rise in euphotic zone ammonium concentrations to a depth averaged ~ 0.3 µM (Fig. 6). In these areas the euphotic zone ammonium concentrations also showed considerable variation with depth (Fig. 7, station 49) but often tended to be greater than nitrate at latitudes between 29 and 32°S. The longitudinal section (Fig. 10) along the shelf edge shows these latitudes to overlap with the peak in chl*a* concentrations between 28 and 34°S.

At the far southern end of the western continental shelf the oceanography was again quite complex. There was a cold core eddy near 114°E with drifter in it (Fig. 3) and considerable meandering by the LC which was still evident as an increase in sea surface temperature relative to ~ 21.2°C (Fig. 3). Shoreward of the LC the surface temperature dropped to 20.2°C and the mixed-layer extended all the way to the seafloor while the rate of vertical mixing was relatively high (Fig. 12 and 5, respectively). At these near shore locations the concentrations of NO_3 were unusually homogeneous with 0.86 µM, the greatest surface concentration observed throughout the voyage, found at the shallowest station (~ 50m, Fig. 12). Surface silicate concentrations were also high but across the entire transect (n = 8) where they averaged 2.11 ± 0.1 (SD) µM. The near-shore depth-averaged (0 to 41 m) N:Si ratios were also high (0.43, SD = 0.030) and consistent with the values found under the core of the LC. The near shore dissolved oxygen concentrations were close to saturation at 228 µM suggesting they must have become oxygenated.

Discussion

Unlike most eastern boundary currents the LC arises in the tropics and is warm, fresh, buoyant, geostrophically-driven and poleward flowing. During winter the LC is easily identifiable as a ~ 50 to 100m deep layer of uniform temperature and salinity with high silicate, phytoplankton and low DIN moving rapidly southward off the west coast of Australia. In spite of its apparently low DIN the peak in LC flow coincides with a shelf scale bloom over ~ 500000 km^2 (Moore et al. 2007). The source of nitrogen to fuel the annual shelf-scale bloom has been hypothesized to be from the pool of dissolved inorganic nutrients found below the seasonal thermocline and brought into the euphotic zone via enhanced vertical mixing possibly associated with autumnal deepening of the surface mixed layer (Feng et al. 2009). More LC flow during La Niña years (positive SOI) is associated with increased fisheries production (Caputi 2008, Caputi et al. 2001) and greater phytoplankton biomass (Koslow et al. 2008) along the west Australian coast. Based on 40 years of monthly data on the continental shelf the warmer water during winter is correlated with greater nitrate concentration (Thompson et al. 2009), a trend that is the reverse of those found in most other locations (Switzer et al. 2003).

During the 2007 cruise there was no evidence that deep mixing into the seasonal thermocline was the dominant mechanism suppling nutrients to eddies or the euphotic zone south of 23°S. On the contrary the most likely source of nutrients to support the Australian west coast bloom was a thin layer of water with low dissolved oxygen and high nitrate concentrations (LDOHN) immediately under the core of the Leeuwin Current. A similar thin layer of low DO at about 200m has been reported in the Indian Ocean from 0 to 25°S at 75E (Wyrtki 1971, Warren 1981), by Rochford (1969) at 110°W and under the northern region of the LC by Woo and Pattiaratchi (2008). Offshore of NW Australia this LDOHN layer was found as shallow as 50m and well separated from the nitrate found below the seasonal thermocline by depth and substantial differences in density (herein). Similarly, at low latitudes, the low DO layer was clearly distinct from water above by very strong gradients in temperature, salinity and fluorescence (herein, Woo and Pattiaratchi 2008). Within the

LDOHN layer the apparent oxygen utilization was stoichometrically sufficient to provide the observed concentrations of nitrate and suggests relatively high and rapid rates of POM decomposition may supply this DIN. The very sharp gradients in physical and biogeochemical parameters indicate very little vertical mixing at these lower latitudes. Although we did not measure these POM to DIN fluxes the physical arrangement of high chl*a* just above the low DO, high DIN layer makes it feasible that local phytoplankton represent the source of POM undergoing decomposition and remineralisation. Alternatively the POM or DIN may have accumulated in this layer over time and have being funnelled into the base of the LC. At 23°S the LC flows south at 0.6 m s^{-1} but the shallowest LDOHN layer was just underneath the core of the LC between 50 and 100m and was moving at one third the velocity (E. Weller, pers. comm.). The California Current (Ward et al. 1989) also has layers of LDOHN but the geographic extent and the high concentrations of nitrate within this relatively shallow N recycling layer observed off Western Australia appear unprecedented. That the thin LDOHN layer was broadly present underneath the LC off NW Australia and then southward under the LC provides a novel explanation for the shelf scale phytoplankton bloom and the other ecological impacts of the variation in LC strength.

Thin layers of nitrite have been reported near the base of the chl*a* maxima with some controversy regarding whether it is due to excretion by phytoplankton or the slow conversion of nitrite to nitrate (Lomas and Lipschutz 2006). The relatively low concentrations of NH_4 and NO_2 observed off north western Australia may be an artefact of relatively sparse bottle sampling which could miss a very thin layer; or unusually efficient nitrification. The lack of observed NO_2 and NH_4 plus the near balance between the apparent oxygen utilization and NO_3 pool favours the latter, efficient conversion of POM into nitrate; e.g. POM → NH_4 → NO_2 → NO_3. We suggest the strong vertical structure allows a highly-structured and tightly-coupled community of amonifiers and nitrifiers to develop under favourable conditions, with sufficient POM near the base of the euphotic zone but still in warm conditions. Thin layers of biota have been reported in a range of ecosystems including coastal shelves (Cowles & Desiderio 1993), fjords (Holliday et al. 1998, Dekshenieks et al. 2001), and open ocean waters (Bjornsen & Nielsen 1991, Carpenter et al. 1995) but there is relatively little known about the vertical distributions of nitrifying bacteria and Archea or Crenoarchaeota (Beman et al. 2008, 2010). The magnitude and speed of the proposed N cycling implies Crenoarchaeota for ammonification (Francis et al. 2005) and the reduction in DO with the paucity of NH_4 or NO_2 suggests the possibility of heterotrophic Crenoarchaeota for the nitrification step (Wuncher et al. 2008). As in other instances of shallow water nitrification the nitrate produced is suggested to be an important source of N for primary production (Wankel et al. 2007). The first survey of ammonium concentrations off the west Australian coast (herein) showed NH_4 concentrations were generally lower than NO_3 with only a few localized exceptions.

Warm core eddies are most often low in biomass and productivity (Biggs 1982) but off west Australia they are have more biomass and are more productive than surrounding waters (Thompson et al. 2007). Based on modelling and satellite data the source of nutrients for these eddies has been suggested to be from the coastal zone (Dietz et al. 2009). The data presented here demonstrate that in 2007 there was no source of coastal zone water with low DO, sufficient nitrate or suitable N:Si ratio to supply these eddies; nor did there appear to be any offshore source of water with these characteristics. Deeper waters in the region do have the right characteristics but remain well isolated from the surface mixed layer of the WC eddies by strong density gradients and there was relatively little evidence that significant 'pumping' occurred from below the seasonal thermocline (McGillicuddy and Robinson 1997). Mixing into the thin layer under the core of the LC seems to be the most likely source of nitrate for the eddies observed at 22 and 31°S.

South of 28°S the surface layer of the LC has become considerably denser (both cooler and saltier) and in some instances appears to have mixed through the deeper LDOHN layer. In 2007 this newly formed and deeper surface mixed layer meandered westward to form a high-biomass warm-core eddy containing significant DIN in the surface mixed layer (herein). A similar process was observed in 2006 (Paterson et al. 2008) and these eddies are more productive than the surrounding water masses (Thompson et al. 2007). As the LC pushed past 28°S it carried elevated DIN as nitrate and ammonium plus ~ 0.3 μg chl*a* L^{-1} within the euphotic zone. Elementary stoichometry would suggest this DIN was sufficient to double or triple the existing standing stock of chl*a* and therefore support the observed annual phytoplankton bloom off Perth (~ 32°S). At these higher latitudes the LC was sometimes mixed deeply enough to entrain the LDOHN layer but it could also contain this layer within the euphotic zone. Either scenario provides an answer why warmer winter waters are associated with a rise in surface nitrate concentrations from ~ 0.1 to 0.3 µM at Rottnest Island (55m depth, 32.2°S, Thompson et al. 2009).

The deepening of the LC south of 28°S was associated with intense horizontal flow, high latent heat loss, high eddy kinetic energy (Feng et al. 2003) and more intense vertical mixing. These processes can generate considerable phytoplankton patchiness (Abrahams 1998). Along the LC from 22 to 34°S the variation in vertical mixing rates estimated from photoprotective pigments was largely sub mesocale. Seasoar sections showed much greater small scale variability than previously reported for the LC (e.g. Woo and Pattiaratchi 2008). The distributions of phytoplankton biomass from onshore to offshore showed biological responses were occurring along the edges of the current flow (e.g. Levy et al. 2001) suggesting mixing along isopycnal edges of the LC flow. The hypothesized small scale of this vertical mixing provides a possible explanation for the patchiness of the biological responses observed off the west coast (e.g. Hanson et al. 2005).

South of 28°S there was a broad rise in euphotic zone ammonium concentrations. The shift from nitrate to ammonium as the primary source of DIN in the water column between 29 and 32°S (excluding the WC eddy) indicates some considerable change in the relative importance of the major pathways of N cycling at these latitudes. It is suggested that an increase in vertical mixing may disrupt the tight coupling between the microbial communities that undertake both ammonification and nitrification within the LDOHN layer in this region. Further south, off the southwest corner of Australia, there was elevated nitrate present throughout the water column. The source of this DIN cannot be ascribed with certainty as the water masses below 34°S were not characterised. The surface flow was northward and it is possible the Capes Current was flowing inside of the LC (Gersbach et al. 1999, Hanson et al. 2005) or a large recirculation due to the presence of a mesoscale eddy. The temperature, salinity, nitrate and silicate characteristics of the water suggests the shelf was flooded with LC water that had been mixed to a depth of ~ 130m before being pushed onto the shelf.

In conclusion, the discovery of a thin layer of high nitrate and low DO (LDOHN) water underneath the core of the LC provides a novel explanation for the shelf scale phytoplankton bloom along the west coast of Australia. The available evidence suggests a shallow, warm and buoyant LC creates conditions that favour rapid and shallow nitrification. The ultimate source of the organic matter used in this remineralisation remains unresolved.

Acknowledgements

We acknowledge funding support from the Marine National Facility (MNF) for vessel time, the Western Australia Marine Science Institution, the Commonwealth Scientific Industrial Research Organization through the Wealth from Oceans Flagship, the University of Western Australia and Murdoch University. We thank David Griffin for the satellite imagery, two anonymous reviewers for their constructive input, the officers and crew of the RV *Southern Surveyor* for their contributions and the MNF hydrochemists for the analysis of nutrient samples. Some analyses used in this study were produced with the Giovanni online data system, developed and maintained by the NASA GES DISC.

ACCEPTED MANUSCRIPT

References

Abraham, E.R., 1998. The generation of plankton patchiness by turbulent stirring. Nature, 391: 577–580.

Armstrong, F.A.J., 1951. The determination of silicate in seawater. J. Mar. Biol. Assoc. U.K.30 (1), 149–160.

Beman, J.M., Popp, B.N., Francis, C.A., 2008. Molecular and biogeochemical evidence for ammonia oxidation by marine Crenarchaeota in the Gulf of California. ISME J. 2, 429–441.

Beman, J.M., Sachdeva, R., Fuhrman, J.A., 2010. Population ecology of nitrifying Archaea and Bacteria in the Southern California Bight. Environmental Microbiology 12 (5), 1282–1292.

Biggs, D.C., 1992. Nutrients, Plankton, and Productivity in a Warm-Core Ring in the Western Gulf of Mexico, J. Geophys. Res., 97(C2), 2143–2154.

Bjornsen, P.K., Nielsen, T.G., 1991. Decimeter scale heterogeneity in plankton during a pycnocline bloom of *Gyrodinium aureolum*. Mar Ecol Prog Ser 73, 263–267.

Brunet, C., Casotti, R., Aronne, B., Vantrepotte, V., 2003. Measured photophysiological parameters used as tools to estimate vertical water movements in the coastal Mediterranean. Journal of Plankton Research 25 (11), 1413–1425.

Caputi, N., 2008, Impact of the Leeuwin Current on the spatial distribution of puerulus settlement of the western rock lobster (*Panulirus cygnus*) and implications for the fishery of Western Australia. Fish. Oceanogr. 17 (2), 147–152.

Caputi, N., Chubb, C., Pearce, A. 2001. Environmental effects on recruitment of the western rock lobster, *Panulirus cygnus*. Mar. Freshw. Res. 52 1167–1174. doi:10.1071/MF01180

Carpenter, E.J., Janson, S., Boje, R., Pollehne, F., Chang J., 1995. The dinoflagellate *Dinophysis norvegica*: biological and ecological observations in the Baltic Sea. Eur J Phycol 30 (1), 1–9.

Claustre, H., Kerherve, P., Marty, J-C., Prieur, L., 1994. Phytoplankton photoadaptation related to some frontal physical processes. J. Mar. Systems 5 (3-5) 251-265.

Condie, S.A., Dunn, J.R., 2006. Seasonal characteristics of the surface mixed layer in the Australasian region: implications for primary production regimes and biogeography. Mar. Freshw. Research 57 (6) 569-590.

Cowles, T.J., Desiderio, R.A., 1993. Resolution of biological microstructure through in situ fluorescence emission spectra. Oceanography 6 (3), 105–111.

Dekshenieks, M.M., Donaghay, P.L., Sullivan, J.M., Rines, J.E.B., Osborn, T.R., Twardowski, M.S. 2001. Temporal and spatial occurrence of thin phytoplankton layers in relation to physical processes. Mar Ecol Prog Ser 223, 61–71.

Dietz, H., Matear, R., Moore, T., 2009. Nutrient supply to anticyclonic meso-scale eddies off western Australia estimated with artificial tracers released in a circulation model. Deep-Sea Research I 56 (9), 1440-1448.

Falkowski, P.G., 1983. Light-shade adaptation and vertical mixing of marine phytoplankton: A comparative field study. J. Mar. Research 41 (2) 215-237.

Fang, F., Morrow, R. 2003. Evolution, movement and decay of warm-core Leeuwin Current eddies. Deep-Sea Research II 50 (12-13), 2245-2261.

Feng, M., Meyers, G.A., Pearce, A.F., Wijffels, S.E., 2003. Annual and interannual variations of the Leeuwin Current at 32°S. J. Geophys. Research, 108 (C11), 3355 doi:10.1029/2002JC001763.

Feng, M., Wijffels, S., Godfrey, S., Meyers, G., 2005. Do eddies play a role in the momentum balance of the Leeuwin Current? Journal of Physical Oceanography, 35(6), 964-975.

Feng, M., Waite, A., Thompson, P.A., 2009. Climate variability and ocean production in the Leeuwin Current system off the west coast of Western Australia. Journal of the Royal Society of Western Australia. 92, 67-81.

Fraga, F., Rios, A.F., Perez, F.F., Figueiras, F.G., 1998. Theoretical limits of the oxygen:carbon and oxygen: nitrogen ratios during photosynthesis and mineralization of organic matter in the sea. Scientia Marina 62 (1-2), 161-168.

Francis, C.A., Roberts, K.J., Beman, J.M., Santoro, A.E., and Oakley, B.B., 2005. Ubiquity and diversity of ammonia oxidizing archaea in water columns and sediments of the ocean. Proc Natl Acad Sci USA 102 (41), 14683–14688.

Garcia, H.E., Gordon, L.I., 1992. Oxygen solubility in seawater: better fitting equations. Limnol. Oceanogr. 37

(6), 1307–1312.

Gersbach, G.H., Pattiaratchi, C.B., Ivey, G.N., Cresswell, G.R., 1999. Upwelling on the south–west coast of Australia — source of the Capes Current. Continental Shelf Res 19 (3), 363–400.

Greenwood, J.E., Feng, M., Waite, A.M., 2007. A one-dimensional simulation of biological production in two contrasting mesoscale eddies in the south eastern Indian Ocean. Deep Sea Research 54 (8-10) 1029-1044.

Hanson, C.E., Pattiaratchi, C.B., Waite, A.M., 2005. Seasonal production regimes off south-western Australia: influence of the Capes and Leeuwin Currents on phytoplankton dynamics. Marine and Freshwater Research 56 (8), 1011-1026.

Holliday, D.V., Pieper, R.E., Greenlaw, C.F., Dawson, J.K., 1998. Acoustical sensing of small-scale vertical structures. Oceanography 11 (1), 18–23.

Huisman, J., van Oostveen, P. and Weissing, F. J. (1999). Critical depth and critical turbulence: Two different mechanisms for the development of phytoplankton blooms. Limnol. Oceanogr. 44 (7), 1781-1787.

Johannes, R.E., Pearce, A.F., Wiebe, W.J., Crossland, C.J., Rimmer, D.W., Smith, D.F., Manning, C., 1994. Nutrient Characteristics of Well-mixed Coastal Waters off Perth, Western Australia, Estuarine, Coastal and Shelf Sci. 39 (3), 273-285.

Johnson, K.S., Coletti, L.J., 2002. In situ ultraviolet spectrophotometry for high resolution and long-term monitoring of nitrate, bromide, and bisulfide in the ocean. Deep Sea Research I, 53 (3), 561-573.

Kamykowski D., Zentara, S.J., 1985. Nitrate and silicic acid in the world ocean: patterns and processes, Mar. Ecol. Prog. Ser. 26, 47–59.

Kérouel, R., Aminot, A., 1997. Fluorometric determination of ammonia in sea and estuarine waters by direct segmented flow analysis. Mar. Chem. 57 (3-4), 265-275.

Koslow, J.A., Pesant, S., Feng, M., Pearce, A.F., Fearns, P., Moore, T., Matear, R., Waite, A., 2008. The effect of the Leeuwin Current on phytoplankton biomass and production off Southwestern Australia. J. Geophys. Research, 113, (C7), C07050. doi:10.1029/2007JC004102.

Levy, M., Klein, P., Treguier, A.M., 2001. Impact of submesoscale physics on production and subduction of phytoplankton in an oligotrophic regime. J. Mar. Res. 59 (4), 535–565.

Litchman, E., Klausmeier, C.A., 2001. Competition of phytoplankton under fluctuating light. Am. Nat. 157 (2), 170–187.

Litchman, E., Klausmeier, C.A., Bossard, P., 2004. Phytoplankton nutrient competition under dynamic light regimes. Limnol. Oceanogr. 49 (4) 1457-1462.

Lomas, M.W., Glibert, P.M., 1999. Interactions between NH4+ and NO3- uptake and assimilation: comparison of diatoms and dinoflagellates at several growth temperatures. Mar. Biol. 133: 541-551.

Lomas, M.W., Lipschultz, F., 2006. Forming the primary nitrite maximum: Nitrifiers or phytoplankton. Limnol. Oceangr. 51 (5), 2453-2467.

Lourey, M.J., Dunn, J.R., Waring, J., 2006. A mixed-layer nutrient climatology of Leeuwin Current and Western Australian shelf waters: seasonal nutrient dynamics and biomass, Journal of Marine Systems 59 (1-2), 25–51.

McGillicuddy, D.J., Robinson, A.R., 1997. Eddy-induced nutrient supply and new production in the Sargasso Sea. Deep-Sea Res. I 44 (8), 1427–1450.

Moline, M.A., 1998. Photoadaptive response during the development of a coastal Antarctic diatom bloom and relationship to water column stability. Limnol. Oceanogr. 43 (1) 146-153.

Moore, T.S., Matear, R.J., Marra, J., Clementson, L., 2007. Phytoplankton variability off the Western Australian Coast: mesoscale eddies and their role in cross-shelf exchange. Deep-Sea Research II, 54 (8-10): 943-960.

Murphy, J., Riley, J.P., 1962. A modified single-solution for the determination of phosphate in natural waters. Analytica chim. Acta 27:31-36.

Parsons, T.R., Maita, Y. and Lalli, C.M., 1984. A manual of chemical and biological methods for seawater analysis. Pergamon: New York, USA. 173pp.

Paterson, H.L., Feng, M., Waite, A.M., Gomis, D., Beckley, L.E., Holliday, D., Thompson, P.A., 2008 Physical and chemical signatures of a developing anticyclonic eddy in the Leeuwin Current, eastern Indian Ocean J. Geophys. Res. 113, C07049, doi:10.1029/2007JC004707.

Pearce, A.F., 1991. Eastern boundary currents of the southern hemisphere. Journal of the Royal Society of Western Australia 74, 35 - 45.

Pearce, A., Pattiaratchi, C., 1999. The Capes Current: a summer countercurrent flowing past Cape Leeuwin and Cape Naturaliste, Western Australia. Continental Shelf Research 19 (3), 401–420. doi:10.1016/S0278-4343(98)00089-2

Polovina, J. J., Howell, E.A., Abecassis, M., 2008. Ocean's least productive waters are expanding, Geophys. Res. Lett., 35, L03618, doi:10.1029/2007GL031745.

Redfield, A.C., 1942. The processes determining the concentration of oxygen, phosphate, and other organic derivatives within the depths of the Atlantic Ocean. Pap. Phys. Oceanogr. Meteor., 9, 1-22.

Rochford, D.J., 1969. Seasonal variations in the Indian Ocean along 110°E. I. Hydrological structure of the upper 500m. Australian Journal of Marine and Freshwater Research. 20 (1), 1-50.

Sprintall, J., Roemmich, D., 1999. Characterizing the structure of the surface layer in the Pacific Ocean. J. Geophys. Res., 104 (C10), 23297–23311.

Switzer, A. C., Kamykowski, D. and Zentara, S-J. 2003. Mapping nitrate in the global ocean using remotely sensed sea surface temperature. Journal of Geophysical Research 108 (c8) 3280-3292. doi:10.1029/2000JC0000444

Thompson, P.A., Baird, M.E., Ingleton, T., Doblin, M.A., 2009. Long-term changes in temperate Australian coastal waters and implications for phytoplankton. Mar. Ecol. Progress Series. 394, 1-19.

Thompson, P.A., Pesant, S., Waite, A.M., 2007. Contrasting the vertical differences in the phytoplankton biology of a warm core versus cold core eddy in the south-eastern Indian Ocean. Deep Sea Research Part II 54 (8-10), 1003-1028.

Thompson, P.A., Waite, A.M., 2003. Phytoplankton responses to wastewater discharges at two sites in West Australia. Mar. Freshw. Research 54 (6), 721-735.

Van Heukelem, L., Thomas, C., 2001. Computer-assisted high-performance liquid chromatography method development with applications to the isolation and analysis of phytoplankton pigments. J. Chromatogr. A 910 (1) 31–49.

Wada, E., Hattori, A. 1971. Nitrite metabolism in the euphotic layer of the central North Pacific Ocean. Limnol. Oceanogr. 16 (5), 766 – 772.

Waite, A.M., Thompson, P.A., Pesant, S., Feng, M., Beckley, L.E., Domingues, C.M., Gaughan, D., Hanson, C.E., Holl, C.M., Koslow, T., Meuleners, M., Montoya, J.P., Moore, T., Muhling, B.A., Paterson, H., Rennie, S., Strzelecki, J. and Twomey, L. (2007) The Leeuwin Current and its eddies: An introductory overview. Deep Sea Research II 54(8-10), 789-796.

Wankel, S.D., Kendall, C. Pennington, J.T., Chavez, F.P., Paytan A., 2007. Nitrification in the euphotic zone as evidenced by nitrate dual isotopic composition: Observations from Monterey Bay, California, Global Biogeochem. Cycles, 21, GB2009, doi:10.1029/2006GB002723.

Ward, B.B., Kilpatrick, K.A., Renger, E.H., Eppley, R.W., 1989. Biological nitrogen cycling in the nitracline. Limnol. Oceanogr. 34 (3), 493-513.

Warren, B.A., 1971. The shallow oxygen minimum of the South Indian Ocean. Deep Sea Research I 28 (8) 859-864.

Woo, L.M., Pattiaratchi, C.B., 2008. Hydrography and water masses off the western Australian coast. Deep-Sea Research I 55 (9), 1090-1104.

Wood, E.D., Armstrong, F.A.J., Richards, F.A., 1967. Determination of nitrate in sea water by cadmium-copper reduction to nitrite. J. Mar. Biol. Ass. U.K., 47 (1), 23-31.

Wood, E.J.F., 1964. Studies in the microbial ecology of the Australasian region. I. Relation of oceanic species of diatoms and dinoflagellates to hydrology. Nova Hedwigia 8 (1-2), 5-20.

Wuchter, C., Abbas, B., Coolen, M.J.L., Herfort, L., van Bleijswijk, J.P.T., Strous, M., Teira, E., Herndl, G.J., Middelburg, J.J., Schouten, S., Sinninghe Damste, J.S., 2006. Archaeal nitrification in the ocean. Proc. Natl Acad. Sci. USA 103 (33), 12317–12322.

Wyrtki, K., 1971: Oceanographic Atlas of the International Indian Ocean Expedition. National Science Foundation Publication, OCE/NSF 86-00-001Washington, DC, 531 pp.

595

Table 1. Correlation coefficients for gradients (Δ) in selected physical, chemical and biological water properties. For each station the change in property (Δ) was calculate from surface to 50 m, from 50 to 100 m and from 100 to 150 m (n = 212 to 214). For each property the *correlation (r^2 value)*, probability (P) value are given in italics, normal text, respectively. Highly correlated properties have similar vertical structure.

	dissolved oxygen	salinity	temperature	% transmission
Fluorescence	*0.0969* 0.160	*-0.208* 0.00231	*0.376* 0.0000000163	*-0.537* 2.3×10^{-17}
Dissolved oxygen		*0.208* 0.00233	*0.0750* 0.277	*-0.135* 0.0494
Salinity			*0.00234* 0.973	*0.219* 0.00136
Temperature				*-0.167* 0.0149

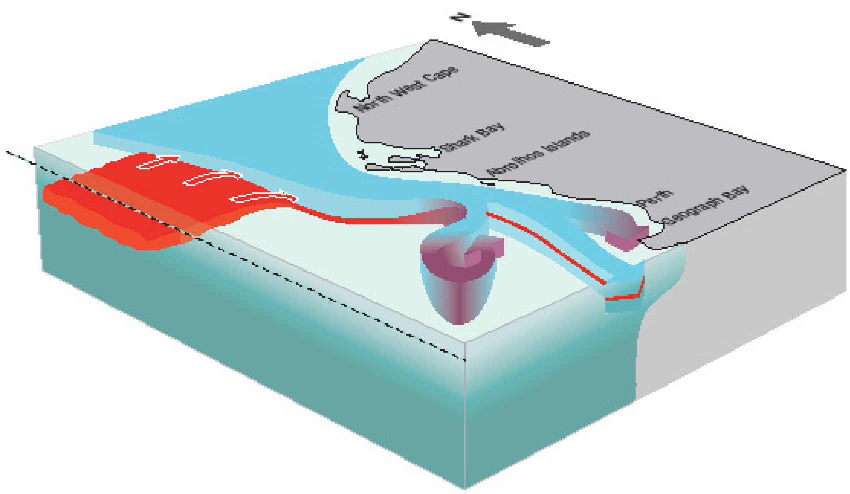

Figure 1. A conceptual representation of the strengthening Leeuwin Current (LC) and entrainment of thin layers of low dissolved oxygen (DO) and high nitrate concentrations as observed during late autumn 2007. At the latitudes of 22 to 25°S the LC is warmer and fresher than surrounding waters with strong vertical gradients in temperature, salinity, oxygen, fluorescence and nitrate observed between 50 and 80 m. Just below this there were thin layers of low DO and high nitrate (red colour). The northern or western extent of these thin layers was not determined but they appear to be entrained into the LC at depth. Southwards and near the Abrolhos Islands the Leeuwin Current narrows along the shelf edge, has cooled, and has high eddy kinetic energy. South of the Abrolhos Islands the LC produced a large warm core eddy observed off the shelf at ~ 31°S with relatively high nitrate (purple colour) and low dissolved oxygen plus N:Si ratios all indicating the source of these waters to result from entrainment of this thin layer into the euphotic zone. Farther south, off Perth (~32°S), the LC existed in 2 modes. One mode with nitrate from this thin layer now mixed to the surface (purple colour) and another with the thin layer still intact but at relatively shallow depths (~

70m).

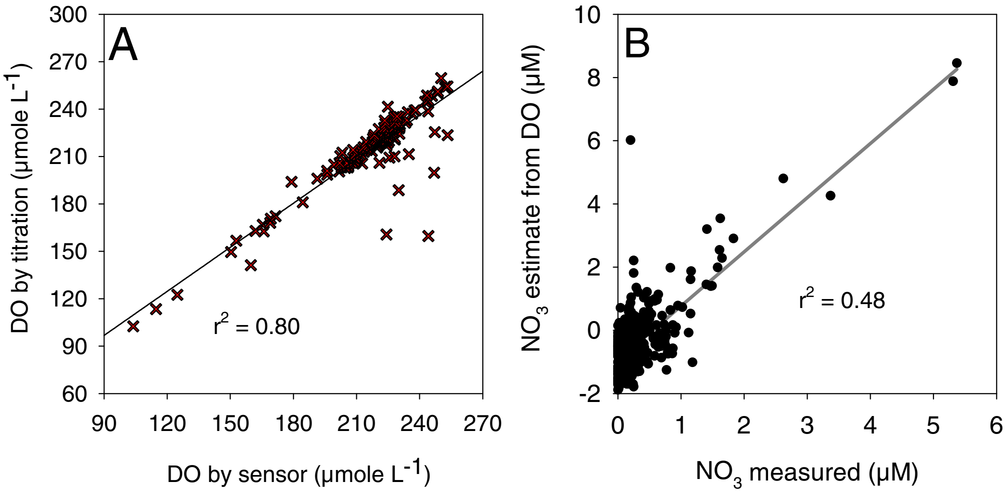

Figure 2. A) Calibration of the dissolved oxygen sensor on the CTD with bottle samples determined by Winkler type titrations. B) Nitrate concentrations measured in bottle samples (x axis) versus potential nitrate concentrations estimated assuming that the oxygen deficit was converted into nitrate at molar ratios of 6.6:6.6:1 for O:C:N.

(colour on web, black and white in print)

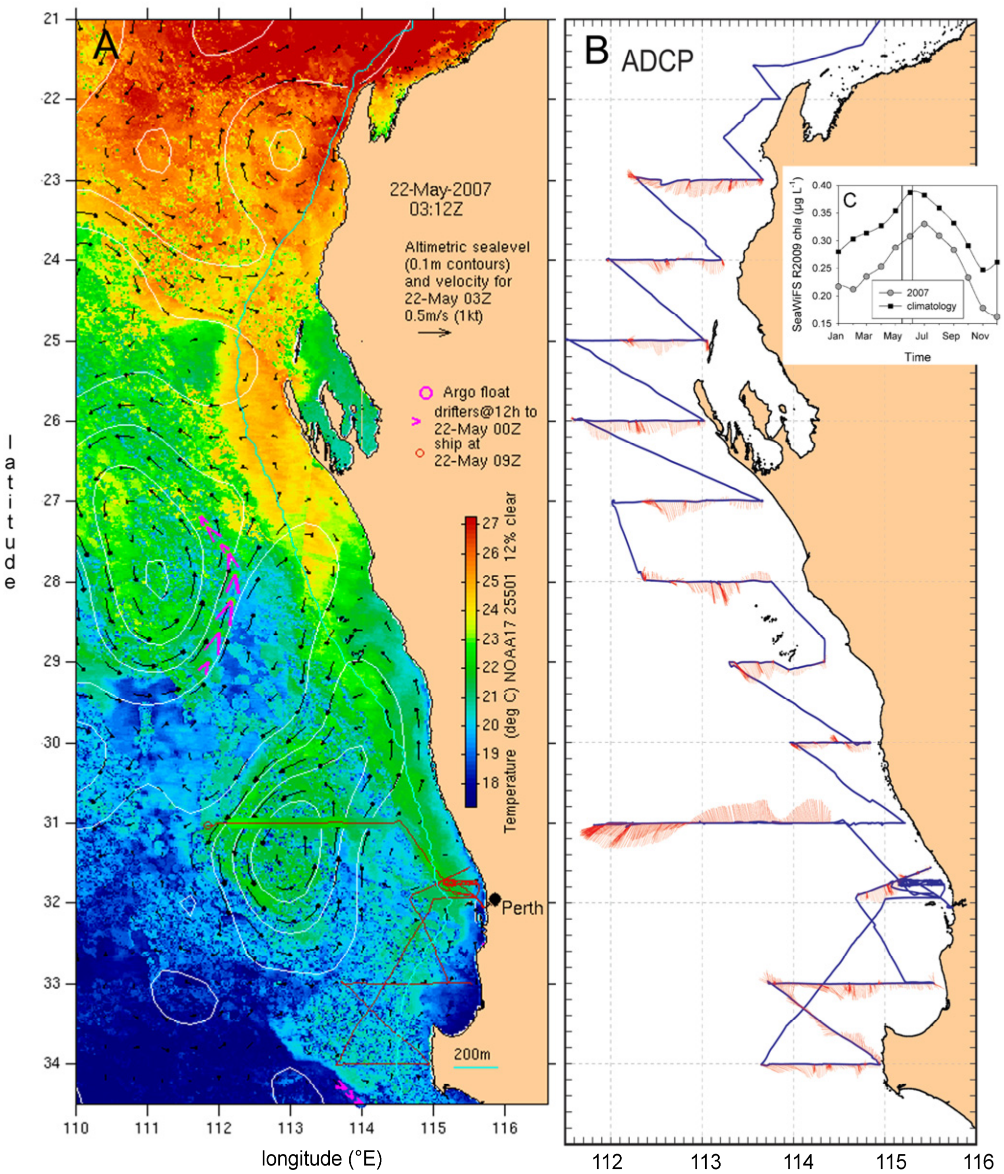

Figure 3. (A) A composite image of sea surface height (white lines at 0.1m contours), sea surface temperature (colours) and current velocities (arrows) estimated from calculated geostrophic flow (David Griffith, pers. comm.) for May 22 2007. (B) Cruise track and shipboard ADCP estimates of current velocities (red arrows) in upper 8m. (C) inset showing seasonal chl*a* from SeaWiFs (R2009) for 2007 and climatology (1997 to 2010) for region in panel B. Cruise duration is shown by solid vertical lines. (print in colour)

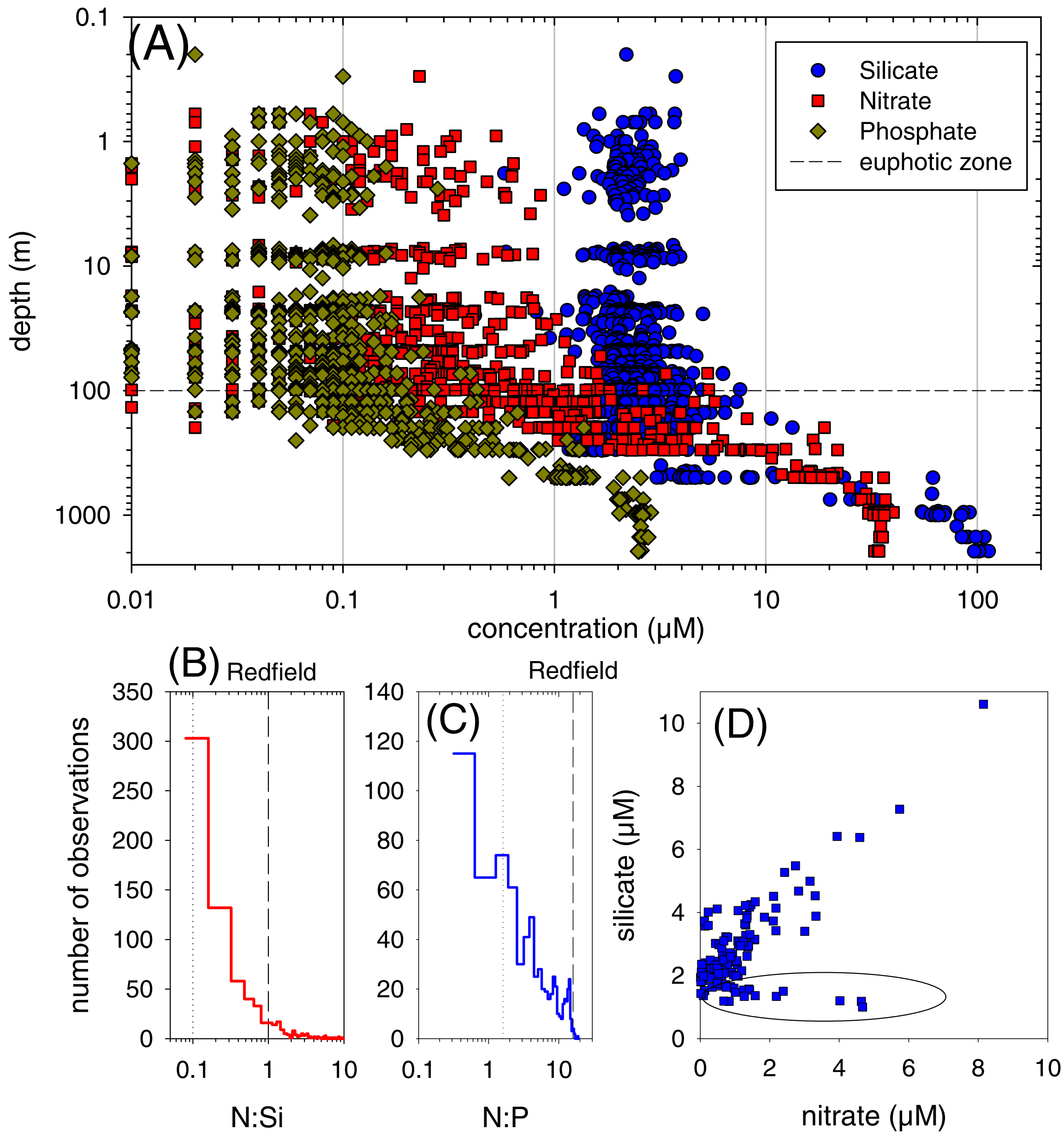

Figure 4. All nutrient concentrations from the entire cruise (Fig. 6B shows locations) over all depths from the surface to 2000 m with just 20 nitrate concentrations above 100m ≥1 µM. Lower panels show histograms for frequency of NO_3:$Si(OH)_4$ or NO_3:PO_4 ratios versus number of observations on $\log_{10}$ scales with dashed vertical lines representing Redfield ratios and dotted lines Redfield/10. Note the majority of samples are greater than 10 times below Redfield indicating the likelihood of severe nitrogen limitation. Lower right panel shows nitrate versus silicate with the unusual combination of high nitrate and low silicate concentrations that are found just under the Leeuwin Current (in the ellipse).

(colour on web, black and white in print)

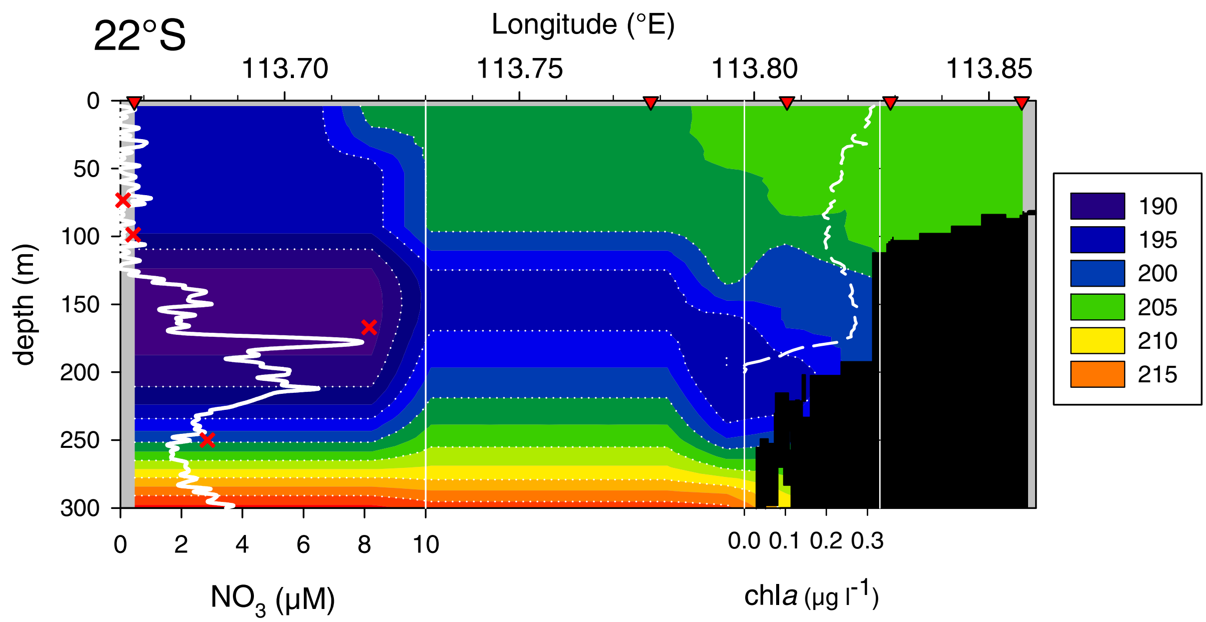

Figure 5. A section at 22°S from near shore to 1000m water depth showing contours for dissolved oxygen (μM). Stations were undertaken at triangles. Solid white line is the vertical profile from nitrate sensor at the offshore station (113.7°E) with concentrations from bottle samples (X). Dashed white line is vertical profile for chl*a* (from calibrated fluorescence) at mid shelf station (113.8°E).

(colour on web, black and white in print)

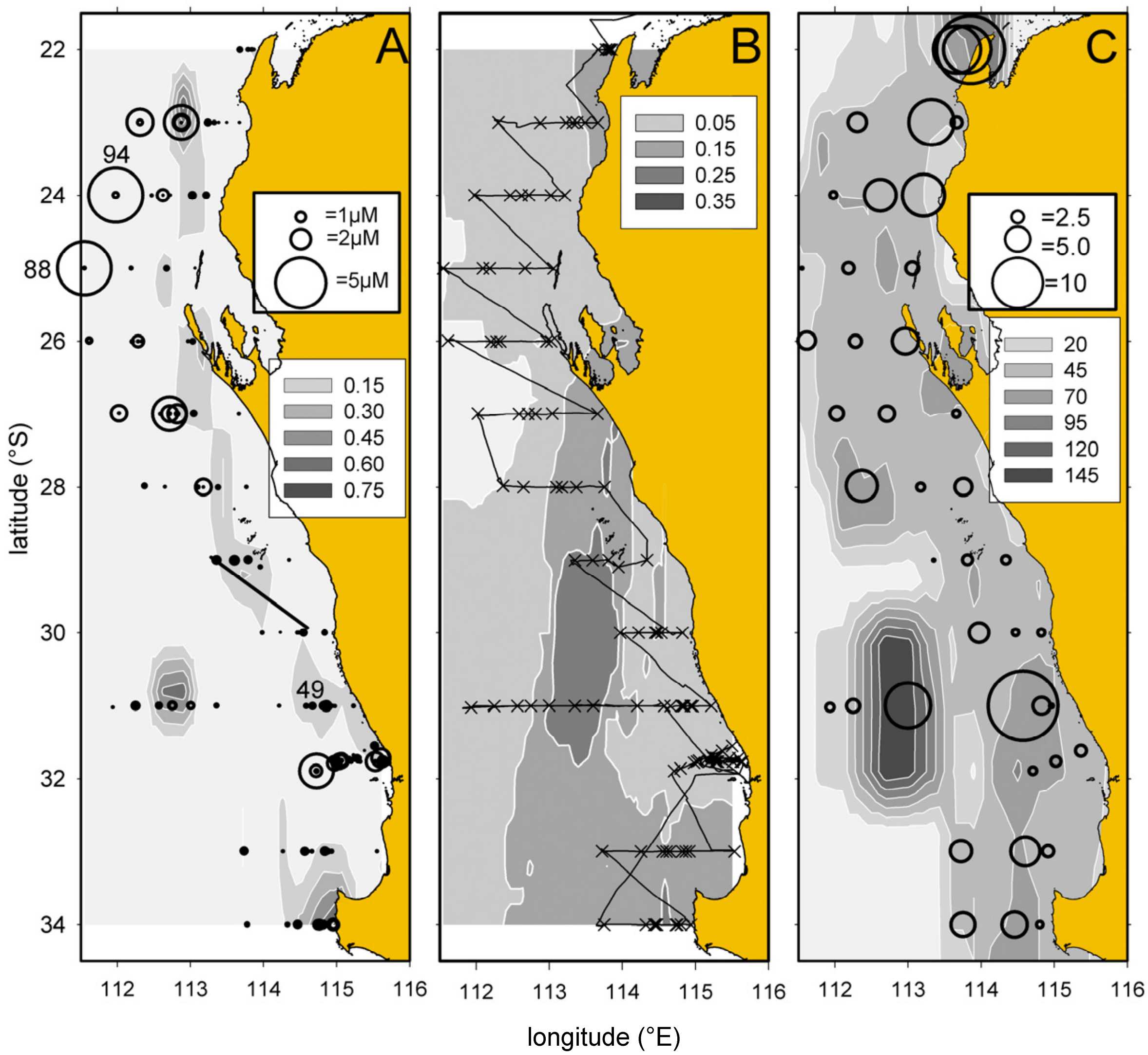

Figure 6. Depth averaged (0 to 100 m) nutrient concentrations from each CTD station, estimated (rates of vertical mixing, cruise track, CTD stations and mixed layer depths. Panel (A) contours for depth averaged (0 – 100m, bottle samples, n ~ 6) nitrate concentrations (µM) and bubble plot of all nitrate concentrations (bottle samples) from 0 to 100 m (bubble size is proportional to concentration). Three specific CTD stations (94, 88, 49) are labelled and shown in detail in Fig 7. Line between 30°S ~ 115°E and 29°S, 113.2°E is seasoar section shown in Fig 8. Panel (B) Cruise track (black line), CTD station locations (thin X), contour plot for depth averaged (0 to 100 m, bottle samples, n ~ 6) ammonium concentrations (µM). Panel (C) Contour plot of mixed layer depths (m)

and bubble plot of estimates of mixing rates (cm s^{-1}) based on ratios of photoprotective pigments

670 (see Material and Methods for details of calculation).

(colour on web, black and white in print)

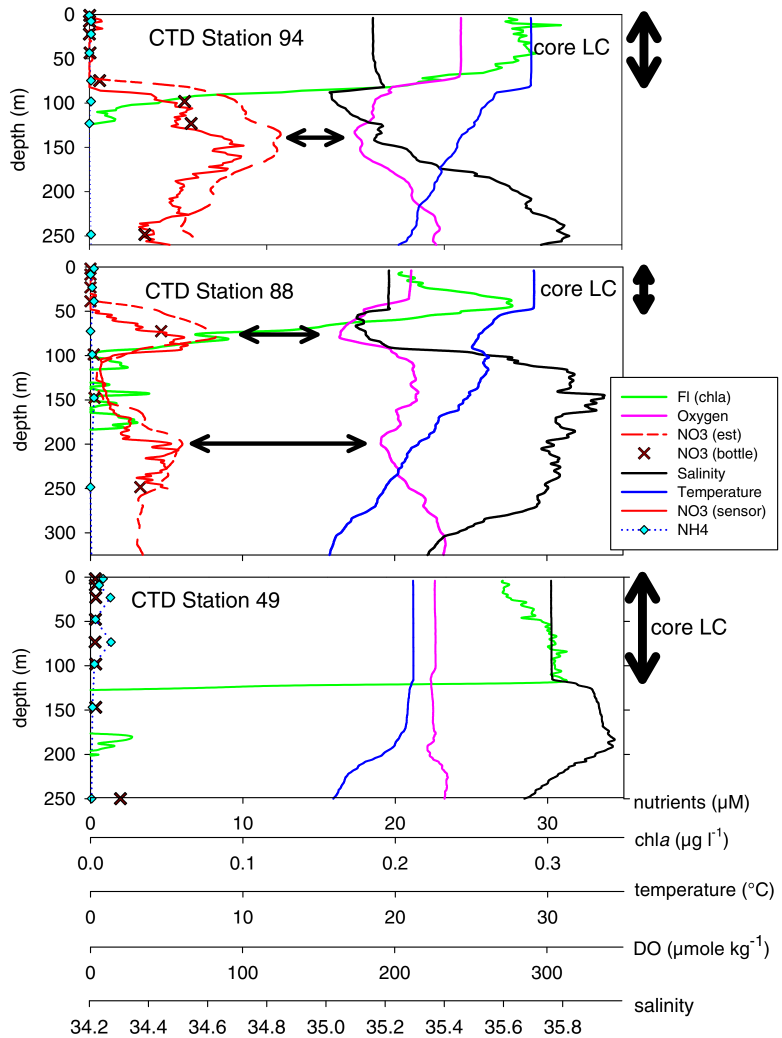

Figure 7. CTD profiles at 24°S (stn 94), 25°S (stn 88) and 31°S (stn 49) see Fig. 6A for locations. All three panels have identical scales. NO_3 estimate is the potential nitrate concentration estimated if apparent oxygen utilization was converted into nitrate at molar ratios of 6.6:6.6:1 for O:C:N. Arrows indicate layers of low dissolved oxygen and high nitrate at relatively shallow depths. At Station 94 there is a broad peak in nitrate and low DO from 100 to 250m. At Station 88 there are similar layers between 50 and 100m and again between 150 and 250m. At Station 49 the LC had deepened to 100m and no layers of low DO & high nitrate were observed. In all instances high fluorescence was observed in the LC.
(colour on web, black and white in print)

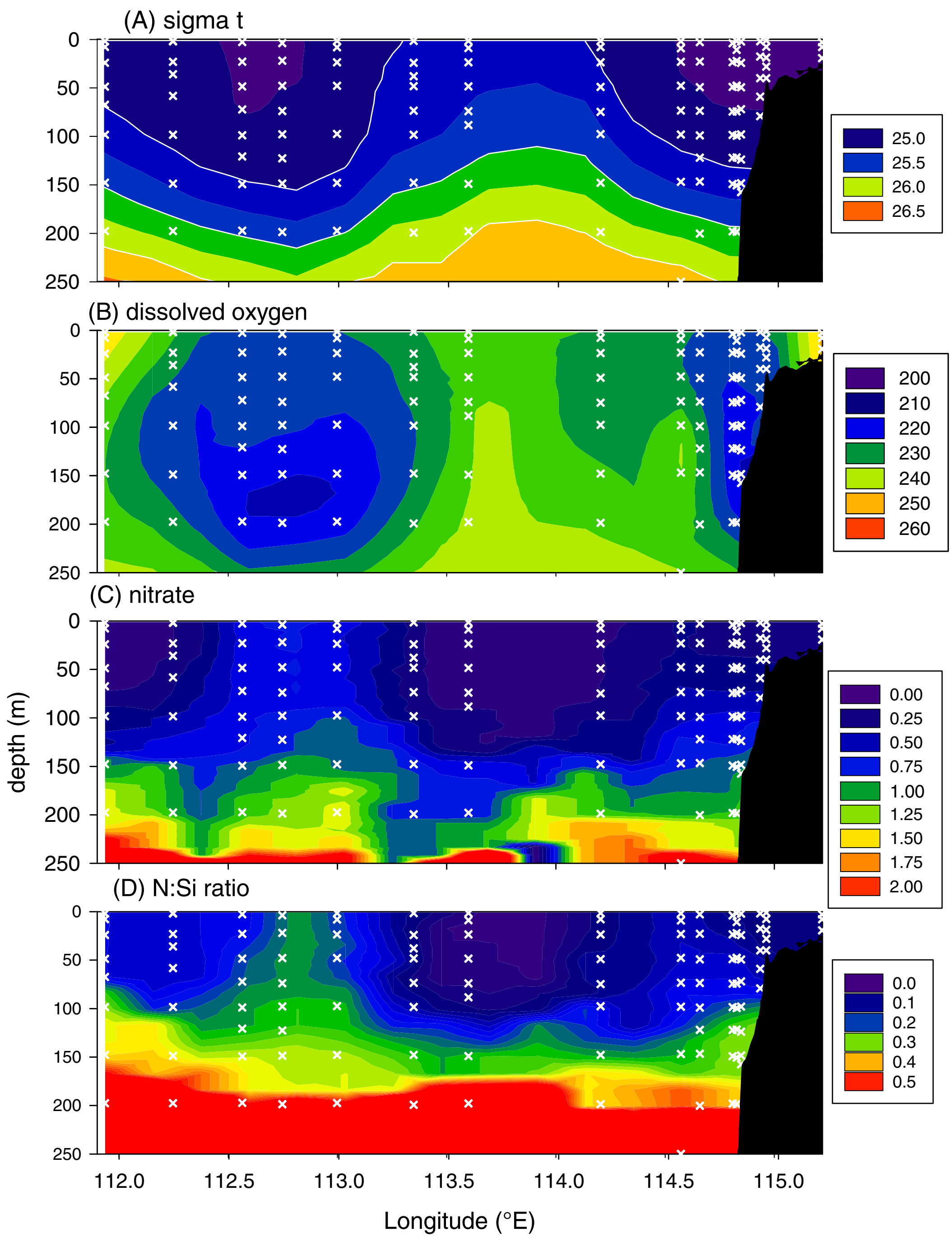

Figure 8. Section along 31°S transect showing (A) buoyant Leeuwin Current water at the shelf edge, ~ 114.8°E; also an eddy at ~ 112.6 °E (density, $sigma_t$ = kg m^{-3} -1000). (B) dissolved oxygen (µM). (C) nitrate (µM from calibrated ISUS sensor). (D) NO_3:$Si(OH)_4$ ratios. The only observed source of water with high nitrate, low dissolved oxygen and high NO_3:$Si(OH)_4$ ratios was ~ 100m deep under the Leeuwin Current upstream of the eddy (white crosses indicate bottle samples and profile location).
(colour on web, black and white in print)

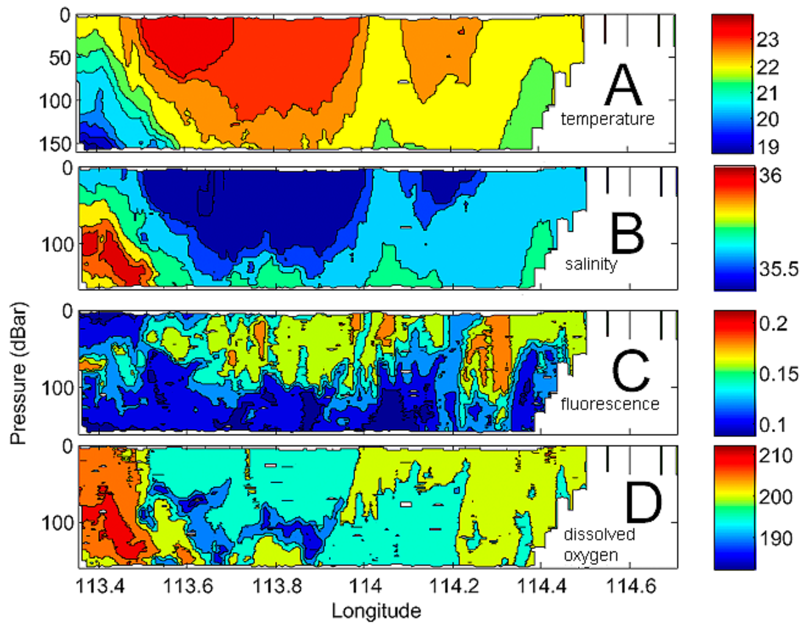

Figure 9. Section composed from hundreds of CTD profiles made by the Seasoar towed from inshore at 30°S 114.6°E to offshore at 31°S 113.3°E (see Figure 6A). (A) is temperature (°C), (B) is salinity, (C) is chl*a* from calibrated fluorescence (D) is dissolved oxygen (µm l^{-1}) from sensor. A layer of low (~ 180 µm l^{-1}) dissolved oxygen between 60 and 120m is clearly evident under the warm water of the Leeuwin Current and discrete from onshore or offshore waters.

(colour on web, black and white in print)

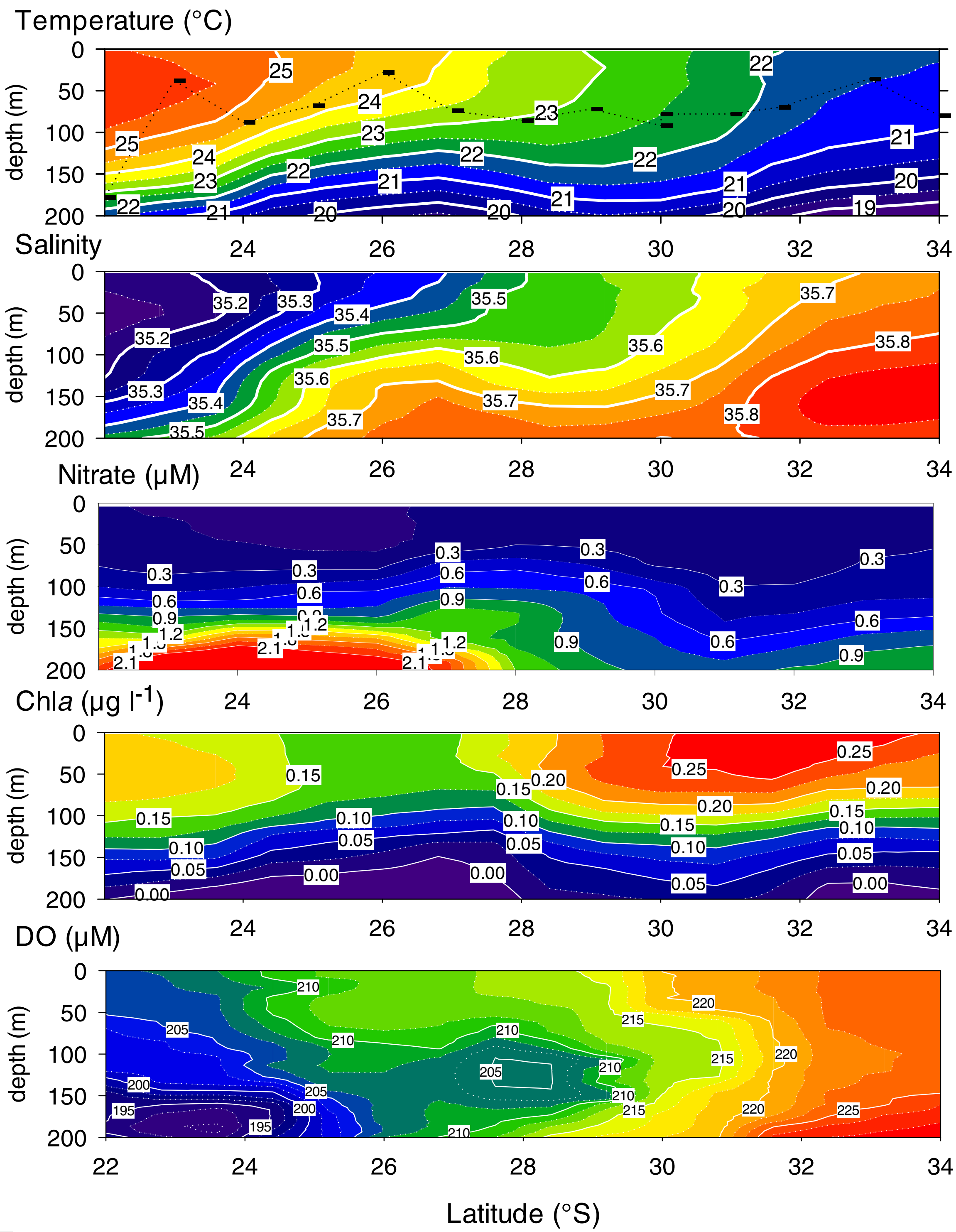

Figure 10. Longitudinal section along continental shelf edge (200 m) showing vertical gradients of temperature, salinity, nitrate, fluorescence (Chl*a*) and dissolved oxygen (DO). One or more vertical profiles at each degree of latitude were used to construct the contours. Top panel shows mixed layer depth at individual stations as a bar (-) and joined by a dotted black line.

(colour on web, black and white in print)

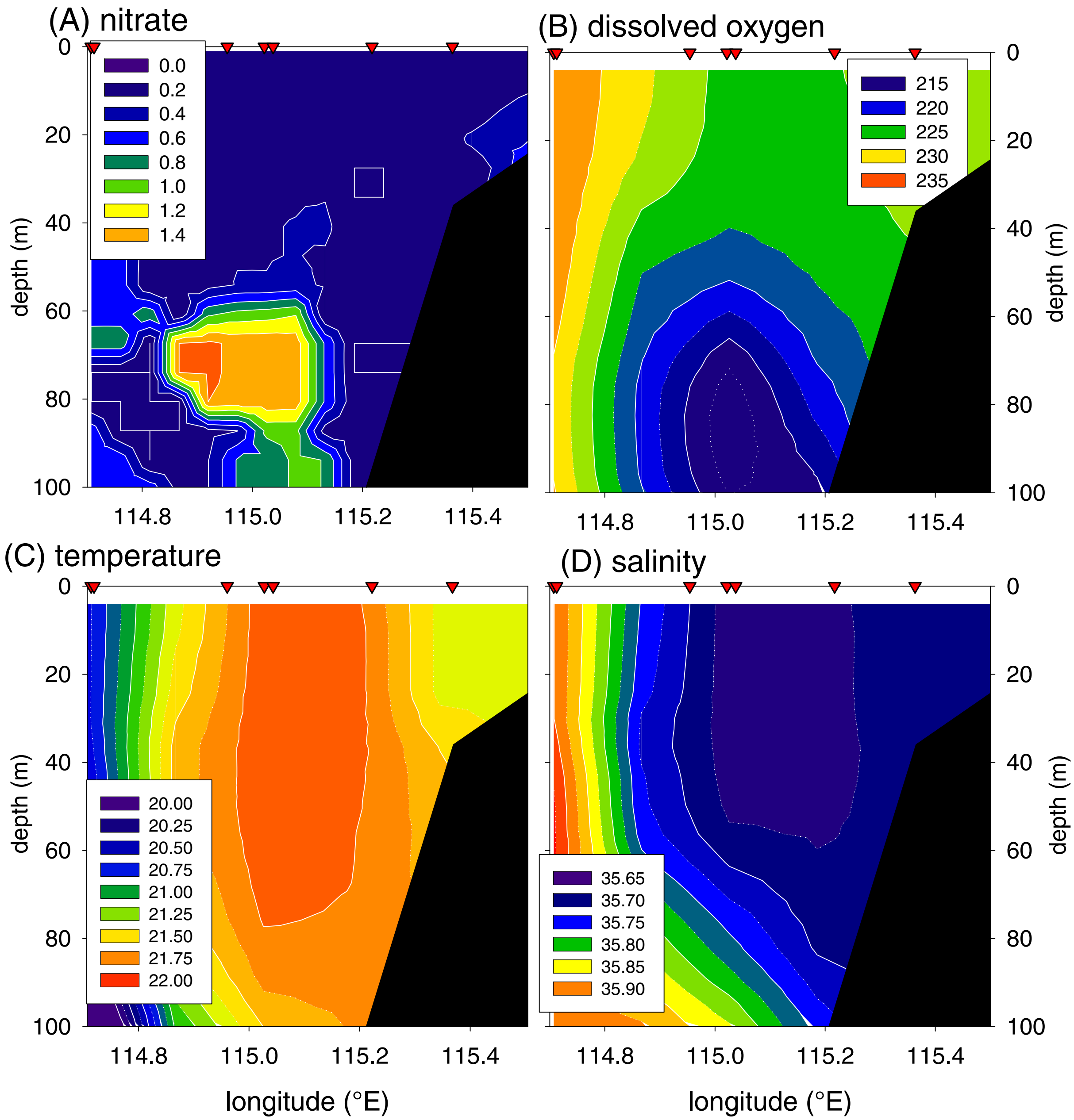

Figure 11. Sections at 32°S from near shore to 1000m water depth. (A) Nitrate section from sensor showing thin layer of high nitrate under core of Leeuwin Current. (B) Dissolved oxygen section with low dissolved oxygen at base of LC, (C) Temperature showing LC generally warmer than inshore or offshore at this latitude, (D) Salinity section showing some modest stratification at ~ 60m depth in the LC. Red triangles indicate locations of CTD profiles.

(colour on web, black and white in print)

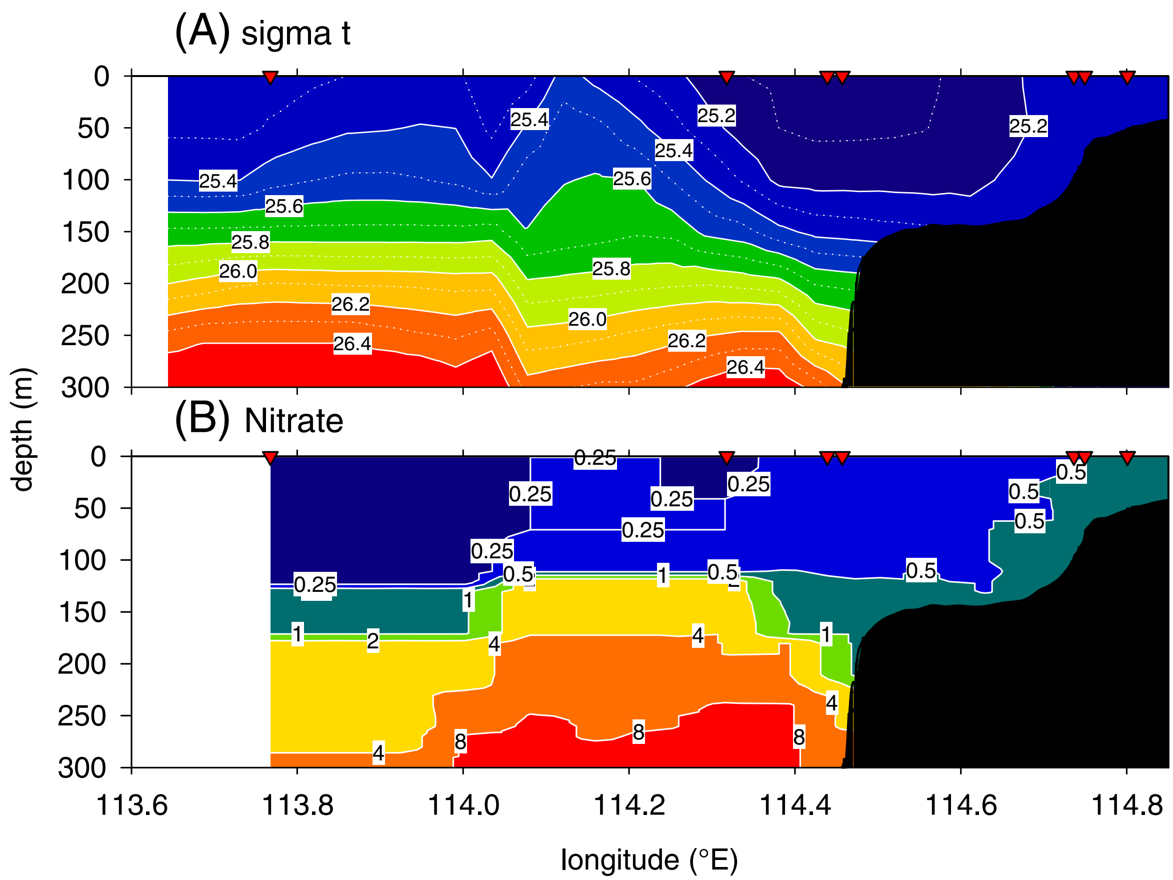

Figure 12. Section at 34°S. (A) shows contoured density (sigma t, density in kg m^{-3} -1000). (B) shows contoured nitrate (μM) from ISUS sensor. Red triangles show locations of CTD profiles.

725

(colour on web, black and white in print)

Research highlights

- Unusually shallow nitrification in eastern Indian Ocean
- Leeuwin Current structure and flow are factors in nitrification
- Shelf scale phytoplankton bloom results from these nutrients
- Anticyclonic eddies in the southeast Indian Ocean derive their nutrients from base of Leeuwin Current